arXiv:0908.0823v1 [astro-ph.CO] 6 Aug 2009

Studying the spectral properties of Active Galactic Nuclei in the JWST era

Th. Nakos, M. Baes

Sterrenkundig Observatorium, University of Ghent, B-9000, Belgium

A. Alonso-Herrero, A. Labiano

Departmento de Astrofísica Molecular e Infrarroja, IEM, CSIC, Madrid, Spain

Abstract

The James Webb Space Telescope (JWST), due to launch in 2014, shall provide an unprecedented wealth of information in the near and mid-infrared wavelengths, thanks to its high-sensitivity instruments and its 6.5 m primary mirror, the largest ever launched into space. NIRSpec and MIRI, the two spectrographs onboard JWST, will play a key role in the study of the spectral features of Active Galactic Nuclei in the $0.6 - 28$ micron wavelength range. This talk aims at presenting an overview of the possibilities provided by these two instruments, in order to prepare the astronomical community for the JWST era.

Key words: Techniques:spectroscopic, quasars:general, Galaxies:active, Galaxies:starburst, early Universe

1. Introduction

The James Webb Space Telescope is a project led by NASA, with major contributions from the European and Canadian Space Agency (ESA, CSA, respectively). Known initially as the Next Generation Space Telescope (NGST), it was renamed in 2002 as the James Webb Space Telescope, after the former NASA administrator. Meant to replace the ageing Hubble Space Telescope (HST), JWST is due to launch in 2014 on an Ariane 5 rocket, from the French Guiana. Its destination will be the semi-stable L2 Lagrange point, some 1.5×10^6 km from Earth. The foreseen life of the mission is five years, although there is a possibility of extension up to ten years.

JWST's primary mirror consists of 18 hexagonal, beryllium-made segments, resulting in a collecting area of $25\,\mathrm{m}^2$. As the size of the mirror (6.5 m diameter), and that of other spacecraft elements, are too large to be accommodated in the rocket shrouds, JWST will be constructed using deployable structures. Thanks to its large aperture and high-sensitivity instruments, JWST is expected to extend the science done with HST not only in terms of performance (higher sensitivity, better resolution) but also in terms of wavelength range. JWST shall be diffraction limited at $2\,\mu$m and its instruments will be performing in the $0.6 - 29\ \mu$m range, limited at the short end by the gold coatings of the primary mirror and at the long end by the mid-infrared (hereafter MIR) detector quantum efficiency. The JWST integrating science instrument module (ISIM) consists of four instruments: a near-infrared camera (NIRCam, Horner & Rieke 2004), a near-infrared spectrograph (NIRSpec, Zamkotsian & Dohlen 2004), a mid-infrared instrument (MIRI, Wright et al. 2004) and a near-infrared tunable filter imager (TFI, Rowlands et al. 2004). A detailed description of the space observatory and its science cornerstones can be found in Gardner et al. (2006).

2. The near-infrared spectrograph (NIRSpec)

NIRSpec is a near-infrared spectrograph, operating in the $0.6-5\,\mu$m wavelength range, with NASA providing the two HgCdTe 2k×2k detectors and the multi-slit system, and ESA the instrument. NIRSpec will be operating in three observing modes:

- Multi-object spectroscopy: thanks to a micro-shutter array (MSA, also provided by NASA), whose elements can either be closed or opened independently, it can simultaneously obtain up to 100 spectra, in a field of view (FoV) of $\approx 3.4 \times 3.4$ arcmin^2.

- Long-slit spectroscopy: six fixed slits (three slits of $3.5'' \times 0.2''$, one $4'' \times 0.4''$ and one $2'' \times 0.1''$) will allow to reach a resolving power between $1000 < R < 2700$ in three spectral bands ($1.0 - 1.8\,\mu$m, $1.7 - 2.9\,\mu$m, $2.9 - 5.0\,\mu$m). Using a single prism, it will also be possible to cover the $0.6 - 5\,\mu$m wavelength range, but at a lower resolution ($R \approx 100$).

- Integral Field Spectroscopy: NIRSpec includes an integral field unit (IFU) with 30 slices, each $0.1''$ wide, with a FoV of $3'' \times 3''$.

The resolution for the different spectroscopic modes is presented in Table 1.

R	Prism/Grating	$\lambda\,(\mu\mathrm{m})$	Mode
100	single prism	$0.6 - 5$	MOS, fixed slit
1000	3 gratings	$1 - 5$	MOS, fixed slit
3000	3 gratings	$1 - 5$	MOS, IFS

Table 1: NIRSpec observing modes: Multi-Object Spectroscopy (MOS), long-slit spectroscopy or Integral Field Spectroscopy (IFS) as a function of spectral resolution.

3. The mid-infrared instrument (MIRI)

MIRI is a European-American collaboration and is unique, in many aspects. First of all, it will be the only instrument operating in the MIR wavelength range $(5 - 28\,\mu\mathrm{m})$. Secondly, it is also the only JWST instrument that can perform imaging, spectroscopy and coronagraphy. MIRI consists of three identical 1024×1024 Si:As sensor chip assemblies (SCA), of $25\,\mu$m pixel size, that shall be operating at $7\,\mathrm{K}$. As the spacecraft will be passively cooled down to $\approx 35\,\mathrm{K}$, the $7\,\mathrm{K}$ temperature will be achieved by means of a mechanical cooler. The MIRI SCAs and cryo-cooler are provided by Jet Propulsion Laboratory, while MIRI's optical system is provided by a consortium of 28 institutes from 10 European countries.

MIRI's imager provides broad and narrow-band imaging, phase-mask coronagraphy, Lyot coronagraphy and low-resolution slit spectroscopy (LRS). The LRS covers the $5 - 10\,\mu$m range with a resolution of $\mathrm{R} \approx 100$ at $7.5\,\mu$m, using a slit width of $0.6''$ and a length of $5.5''$. The imager will have a pixel scale of $0.11''$ and a FoV (excluding the region occupied by the coronagraphs and the LRS) of $79'' \times 113''$.

MIRI's two IFUs will allow to derive spectral and spatial information of the targeted objects with a resolution of $\mathrm{R} \approx 2000 - 3700$ over the $5\,\mu$m $< \lambda < 27\,\mu$m wavelength range. The IFUs provide four simultaneous and concentric FoVs, that increase in size with wavelength. One of the two IFUs will cover the short-wavelength range $(5 - 11.9\,\mu\mathrm{m})$ while the second one will cover the long-wavelength range $(11.9 - 28.3\,\mu\mathrm{m})$. The main properties of the MIRI medium resolution spectrometer (MRS) are presented in Table 2. Fig. 1 shows how MIRI's imager and MRS will be occupying the allocated region of the JWST focal plane.
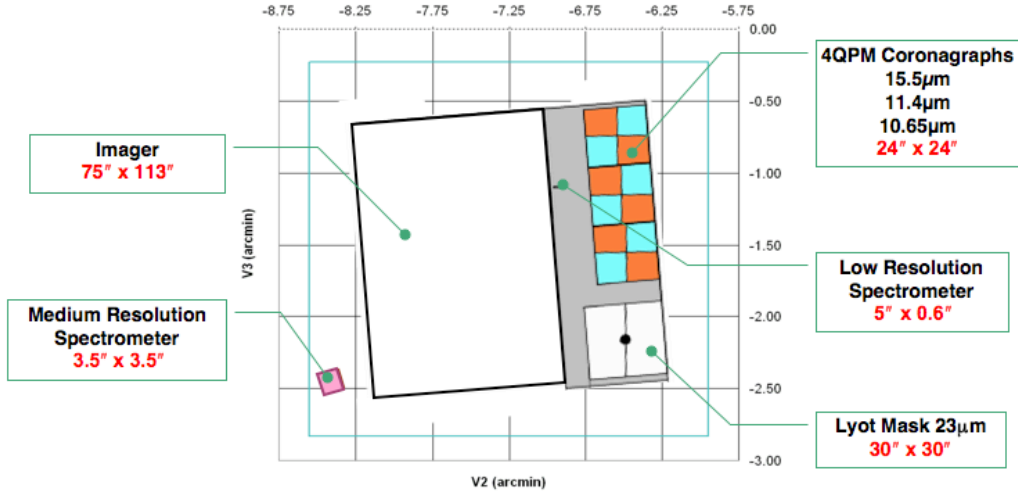
Figure 1: The layout of the MIRI Imager focal plane and the Medium Resolution Spectrometer within the allocated region box) of the JWST focal plane. For the Imager the position of the three four-quadrant phase-mask (4QPM) coronagraphs, of the Lyot stop and of the low-resolution spectrograph, are also visible.

4. NIRSpec and MIRI sensitivity

Thanks to its large mirror, the location from which the observatory will be operating (L2 point) and its high-sensitivity detectors, JWST will be at least 100 times more sensitive than Spitzer and will provide an order of magnitude improved spatial/spectral resolution. More specifically, for NIRSpec, the sensitivity requirements for the R $\approx$ 100 mode is a flux continuum of 132 nJy (AB > 28) at $3.0\,\mu$m for a 10 000 sec exposure and a signal-to-noise ratio of 10; for the R $\approx$ 1000 mode the limiting line-flux will be $\approx 6 \times 10^{-19}$erg s^{-1} cm^{-2} at $2\,\mu$m (Gardner et al. 2006). Regarding MIRI, the requirement sensitivity at 6.4, 9.2, 14.5 and $22.5\,\mu$m for a 10 000 sec exposure and a 10-σ detection is 12.2, 9.9, 11.6 and 59.7×10^{-21}W/m^2, respectively (Swinyard et al. 2004).

5. AGN-related science with NIRSpec & MIRI

Active Galactic Nuclei (AGN) play a major role in astrophysical research, for the following reasons:

- Quasars, the most luminous members of the AGN family, are among the few cosmological light-houses that can probe the lower-end ($z \approx 6 - 7$) of the reionization epoch.

4

λ	Slices	Spatial sample dimens.		FoV		R
μm		Across ($''$)	Along ($''$)	Across ($''$)	Along ($''$)	
$5.0 - 7.7$	21	0.18	0.20	3.7	3.7	$2400 - 3700$
$7.7 - 11.9$	17	0.28	0.20	4.5	4.7	$2400 - 3600$
$11.9 - 18.3$	16	0.39	0.25	6.1	6.2	$2400 - 3600$
$18.3 - 28.3$	12	0.64	0.27	7.9	7.7	$2000 - 2400$

Table 2: Properties of the MIRI integral field units. The region of the sky corresponding to a spatial sample is set by the slice width in the across slice direction, and by the pixel field of view in the along slice direction.

- Non-quasar AGN, detected at lower redshifts ($z < 3$), are a key to understanding the cosmological evolution once the Universe became fully ionized: how galaxies formed, what triggers the black hole (BH) activity, what is the relation between starbursts and AGN, why observations contradict the predictions of the so-called AGN unification scheme.

- The vicinity of the BH is one of the most complex physical laboratories, with electromagnetic radiation being emitted from the X-rays to the far-IR and even radio-waves.

Spectroscopy is indispensable for shedding light on all issues mentioned above. In the following sub-sections we briefly present some of the aspects in which NIRSpec and MIRI will potentially have a major contribution.

5.1. Probing the reionization epoch via high-z quasar spectra

The detection of high-redshift quasars has proven to be a powerful tool for studying the low-end of the reionization epoch (Fan et al. 2006), via the Gunn-Peterson trough (Gunn & Peterson 1965). Quasar-based studies imply that the Universe was opaque (i.e. contained a large fraction of neutral hydrogen) down to $z \approx 6$. On the other hand, CMB polarization studies suggest that the "dark ages" ended at $z_{reion} = 10.9 \pm 1.4$, with the Universe changing instantaneously from neutral to a fully ionized state at this specific redshift (Komatsu et al. 2009).

A possible cause for this discrepancy might be due to (a) the assumptions made for the data analysis or (b) data-related uncertainties. More specifically, difficulties in obtaining robust redshifts estimates, the insufficient precision with which the latter ones are known, and uncertainties on the calculation of the depression of the quasar continuum level based on

Lyα, Lyβ or Lyγ measurements have a direct impact on the models used to describe the reionization process (Fan et al. 2006).

For the case of quasars, the cause of uncertainties can be controlled by improving both the quality and the quantity of the data. The best analysis for measuring the redshift evolution of the Gunn-Peterson optical depth is based on some 19 SDSS quasars at $5.7 < z < 6.4$ (Fan et al. 2006). As the SDSS survey is not optimized for the detection of high-z quasars (due to its wavelength coverage), currently operating (e.g. UKIDSS, Hewett et al. 2006) and forthcoming (VISTA, Emerson et al. 2004) infrared surveys shall identify numerous quasar candidates at high redshift. NIRSpec observations will allow both (a) to confirm (or reject) the nature of the proposed candidates and (b) to study the spectral properties of quasars at $z > 7.2$ (for which the Lyα enters NIRSpec's range), to obtain estimates of the fraction of neutral hydrogen as a function of redshift.

5.2. The AGN unification scheme

Despite its small aperture ($0.8\,\mathrm{m}$), Spitzer has revolutionised our knowledge about AGN: large-area MIR photometric surveys revealed numerous dust-obscured AGN candidates (Lacy et al. 2004; Hatziminaoglou et al. 2005; Stern et al. 2005; Alonso-Herrero et al. 2006; Daddi et al. 2007; Donley et al. 2007), many of which, due to their very red colours, would have otherwise been missed by optical surveys, due to selection biases. A significant fraction of these objects would even be missed by deep, X-ray surveys, due to the very high column densities of ionized gas surrounding the BH. Using ground-based facilities, optical spectroscopic follow-up observations have been done only for the brightest objects (Lacy et al. 2007), as a large fraction of these IR-selected AGN candidates are too faint to obtain spectra with ground-based telescopes.

Selecting AGN using complementary selection criteria is the only way to understand the reason for which the so-called unification scheme (Antonucci 1993) does not work for some 30% of AGN (Garcet et al. 2007, and references therein). According to the unification scheme, the absorption (in X-rays) and extinction (in UV, optical) is a geometrical effect: the absorbing material that surrounds the BH (the putative "torus") might be affecting the observed properties of AGN depending on the viewing angle of the observer with respect to the "torus". Objects with strong X-ray absorption, however, seem to have mild optical and UV extinction (Page et al. 2001), while AGN with narrow emission lines in optical spectra show mild (or even absent)

X-ray absorption (Panessa & Bassani 2002). Finally, there is observational evidence (Punsly 2006) that even challenges the fact that broad absorption line (BAL) quasars are X-ray weak (Gallagher et al. 2006).

MIRI shall be an excellent instrument for studying the characteristics of the obscuring material (that mainly emits in the MIR and FIR), which is the key to understanding the controversy between unified scheme predictions and observations. The $9.7\,\mu$m silicate feature, for example, provides an estimate of the absorption due to the "torus" and can be associated to the column density N_H, a measure of the obscuration that X-rays experience due to the ionized gas (Li & Draine 2001; Shi et al. 2006). High-quality MIR spectra will permit to properly measure the continuum level around this feature and associate it to the flux density for unabsorbed continuum, for objects out to $z \approx 1.9$.

5.3. The starburst - AGN relation

Sensitive observations with Spitzer are showing that AGN are common in infrared bright galaxies at high-z (e.g. Yan et al. 2005; Dey et al. 2008) and especially in massive galaxies (Daddi et al. 2007). However, the relationship between AGN and star formation locally and at high redshift is still not well understood. Mergers and strong interactions are believed to trigger AGN activity in galaxies (Heckman et al. 1986), and these events can also produce instabilities in the ISM and trigger intense episodes of star formation or starbursts (Ho 2005). Nevertheless, it is still not clear how gaseous material is funnelled into the central region of galaxies and what is the relation between star formation and quasar activity. For instance, AGN are located in the transition region (the so-called green valley) between the blue cloud (star-forming galaxies) and the red sequence (quiescent galaxies, see e.g. Nandra et al. 2007), and it has been suggested they may play a role in quenching star formation in galaxies. However, so far it is not clear the role of AGN in quenching or triggering star formation (see, e.g. Alonso-Herrero et al. 2008; Bundy et al. 2008).

The IR spectral range is exceptionally rich in features which can be used to differentiate between AGN activity and star formation, such as (a) PAH features, (b) extended hydrogen recombination line emission, (c) the presence of a strong hot dust continuum and (d) high-excitation and coronal emission lines (see, e.g. Sturm et al. 2002). All these features can be observed with NIRSpec and MIRI for galaxies at different redshifts, and these observations will allow us to unravel the mechanisms responsible for star formation and

AGN activity in galaxies, and understand their evolution as a function of redshift.

References

Alonso-Herrero, et al. 2006, ApJ, 640, 167
Alonso-Herrero, et al. 2008, ApJ, 677, 127
Antonucci, R. 1993, ARA&A, 31, 473
Bundy, K., et al. 2008, ApJ, 681, 931
Daddi, E., et al. 2007, ApJ, 670, 173
Dey, A., et al. 2008, ApJ, 677, 943
Donley, J. L., et al. 2007, ApJ, 660, 167
Emerson, J. P., et al. 2004, The Messenger, 117, 27
Fan, X., et al. 2006, AJ, 132, 117
Garcet, O., et al. 2007, A&A, 474, 473
Gardner, J. P., et al. 2006, Space Science Reviews, 123, 485
Gallagher, S. C., et al. 2006, ApJ, 644, 709
Gunn, J. E., & Peterson, B. A. 1965, ApJ, 142, 1633
Hatziminaoglou, E., et al. 2005, AJ, 129, 1198
Heckman, T. M., et al. 1986, ApJ, 311, 526
Hewett, P. C., et al. 2006, MNRAS, 367, 454
Ho, L. C. 2005, ApJ, 629, 680
Horner, S. D., & Rieke, M. J. 2004, Proceedings of SPIE, 5487, 628
Komatsu, E., et al. 2009, ApJS, 180, 330
Lacy, M., et al. 2004, ApJS, 154, 166
Lacy, M., et al. 2007, AJ, 133, 186
Li, A., & Draine, B. T. 2001, ApJ, 554, 778
Nandra, K., et al. 2007, ApJ, 660, L11
Page, M. J., Mittaz, J. P. D., & Carrera, F. J. 2001, MNRAS, 325, 575
Panessa, F., & Bassani, L. 2002, A&A, 394, 435
Punsly, B. 2006, ApJ, 647, 886
Rowlands, N., et al. 2004, Proceedings of SPIE, 5487, 664
Shi, Y., et al. 2006, ApJ, 653, 127
Stern, D., et al. 2005, ApJ, 631, 163
Sturm, E., Lutz, et al. 2002, A&A, 393, 821
Swinyard, B. M., et al. 2004, Proceedings of SPIE, 5487, 785
Wright, G. S., et al. 2004, Proceedings of SPIE, 5487, 653
Yan, L., et al. 2005, ApJ, 628, 604
Zamkotsian, F., & Dohlen, K. 2004, Proceedings of SPIE, 5487, 635